

Time-series photometry of Earth flyby asteroid 2012 DA₁₄

Tsuyoshi Terai¹, Seitaro Urakawa², Jun Takahashi³, Fumi Yoshida¹, Goichi Oshima⁴, Kenta Aratani⁴, Hisaki Hoshi⁴,
Taiki Sato⁴, Kazutoshi Ushioda⁴, and Yumiko Oasa⁴

¹ National Astronomical Observatory of Japan, 2-21-1 Osawa, Mitaka, Tokyo 181-8588, Japan
e-mail: tsuyoshi.terai@nao.ac.jp

² Bisei Spaceguard Center, Japan Spaceguard Association, 1716-3 Okura, Bisei, Ibara, Okayama 714-1411, Japan

³ Center for Astronomy, University of Hyogo, 407-2 Nishigaichi, Sayo-cho, Sayo-gun, Hyogo 679-5313, Japan

⁴ Faculty of Education, Saitama University, 255 Shimo-Okubo, Sakura, Saitama 338-8570, Japan

Received 28 June 2013 / Accepted 12 September 2013

ABSTRACT

Context. The object 2012 DA₁₄ is a near-Earth asteroid with a size of several tens of meters. It had approached closely the Earth on 15 February, 2013 UT, providing an opportunity for precise measurements of this tiny asteroid.

Aims. The solar phase angle of 2012 DA₁₄ had varied widely around its closest approach but was almost constant during the following night. We performed time-series photometric observations on those two nights to determine the rotational properties and phase effect.

Methods. The observations were carried out using the 0.55-m telescope at Saitama University, Japan. The *R*-band images were obtained continuously over a 2 hr period at the closest approach and for about 5 hr on the next night.

Results. The lightcurve data from the second night indicates a rotational period of $11.0^{+1.8}_{-0.6}$ hr and a peak-to-peak amplitude of 1.59 ± 0.02 mag. The brightness variation before and after the closest approach was separated into two components that are derived from the rotation and phase effect. We found that the phase curve slope of this asteroid is significantly shallower than those of other L-type asteroids.

Conclusions. We suggest that 2012 DA₁₄ is coated with a coarse surface that lacks fine regolith particles and/or a high albedo surface.

Key words. minor planets, asteroids: individual: 2012 DA₁₄ - methods: observational - techniques: photometric

1. Introduction

On February 15, 2013 UT, the near-Earth object (NEO), 2012 DA₁₄, passed closely to the Earth at a distance of about 27,700 km inside a geosynchronous orbit (Włodarczyk 2012). Its diameter was estimated to be probably less than 50 m from the Goldstone radar measurements¹. Since ten-meter sized asteroids are too faint to be observed in detail, their population, internal structure, and surface properties remain uncertain even though these are required for estimating the frequency and influence of hazardous impact events onto the Earth (e.g., Morrison et al. 2002). These small asteroids also have short dynamical/collisional lifetimes and a feeble surface gravity, so that their surface properties and structure could be substantially different from 1–100 km-sized asteroids.

The Earth flyby made 2012 DA₁₄ bright enough to be precisely observed by relatively small telescopes on the ground. This event was an exciting opportunity to investigate the surface properties of such a small asteroid. Its visible/near-infrared colors and visible spectra were already presented by de León et al. (2013) and Urakawa et al. (2013). Interestingly, both studies classified 2012 DA₁₄ as an L-type, a minor taxonomic class among asteroid population. De León et al. (2013) also indicated the rotational period of 8.95 ± 0.08 hr. In this paper, we focus on the relationship between reflectance and solar phase angle, which is known as the photometric phase curve. It provides useful indications of the surface properties, such as geo-

metric albedo and regolith structure. We present the rotational lightcurve and phase curve of 2012 DA₁₄ from our time-series photometric observations around the closest approach and on the next night.

2. Observations and measurements

Our observations have been carried out on the two consecutive nights of February 15 and 16, 2013 (UT). We used the 0.55-m telescope at Saitama University in Saitama, Japan (139.6059° E, 35.8624° N) with the FLI Micro Line ML-4710 CCD (1056 × 1027 pixels) mounted on the prime focus that covers a 32' × 32' field of view (FOV). All images have been taken with sidereal tracking. Before the target crossed the edge of the FOV, we moved the telescope in the same direction that the asteroid moved so that the asteroid would stay in the FOV. Most of the imaging data were continuously obtained over the observations with the Johnson *R*-band. The typical seeing was 3''–4''.

In the first night, the time-series imaging was performed around the closest approach of 2012 DA₁₄ at 19:33 UT over a period of ~2 hr. The asteroid 2012 DA₁₄ moved from the altitude of 18° to 40° with a sky motion of 20–52 arcmin min⁻¹. The solar phase angle decreased from 38° to 19° before 19:55 UT, then increased until 42°. We obtained more than 2,000 images that were taken every 2 sec with a 0.5-sec exposure by using defocus imaging to avoid saturation of the target asteroid. All the images were bias corrected, flat-fielded, and sky subtracted. In spite of the short exposure, the shape of 2012 DA₁₄ images is elongated due to its extremely fast sky motion. Its barycenters

¹ Presented by Lance A. M. Benner at http://echo.jpl.nasa.gov/asteroids/2012DA14/2012DA14_planning.html

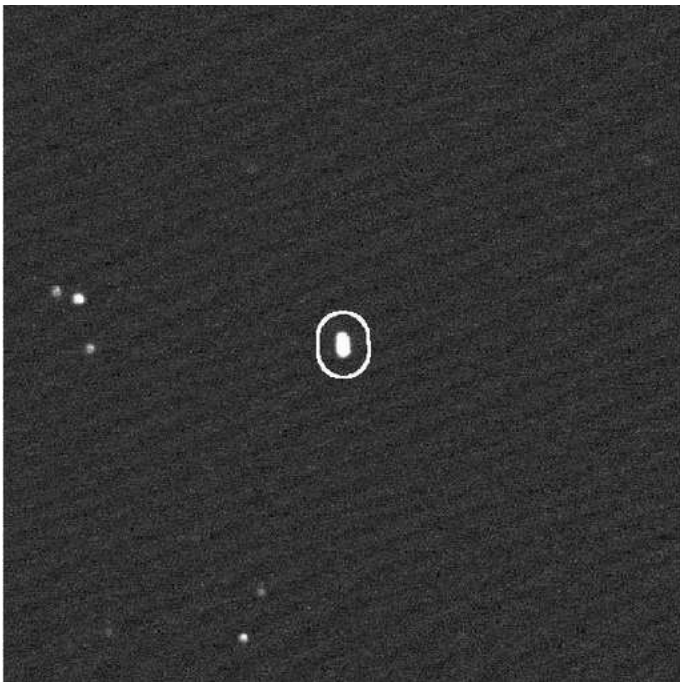


Fig. 1. An R -band image of 2012 DA₁₄ taken by the 0.55-m Saitama University telescope at the closest approach with a 0.5-sec exposure. The field-of-view covers $20' \times 20'$. The solid line represents the moving-circular aperture used for photometry.

may not coincide with the position that coincides with the center of the exposures. This discrepancy could cause an uncertainty of the measured central coordinates. For improving the positioning accuracy, pixel values for light sources on each image were replaced by a constant value substantially that is larger than the sky level. The central coordinates of the asteroid were then determined by ellipse fitting of the processed images. The total flux of the asteroid on each image was calculated based on the total counts within an elongated circular aperture with a radius of $30''$ assuming the synthetic shape of the asteroid image (see Figure 1). If a field star overlaps with 2012 DA₁₄, the data were excluded. Using the field stars identified as USNO-B1.0 stars with an $R < 12$ mag (Monet et al. 2003), the zero magnitude point and atmospheric extinction coefficient were estimated.

During the second night, the identical observation was conducted over ~ 5 hr. However, the exposure times were 10–60 sec because the asteroid became faint ($R \sim 15$ mag) and slow (< 0.3 arcmin min^{-1}) compared to the previous night. The images were corrected with the same reduction processes as the first night data. The brightness variation of 2012 DA₁₄ was measured with relative photometry using ten or more field stars in every sky area. The aperture was the same as that mentioned above but with a radius of $10''$. The Landolt standard stars observed immediately before this photometric sequence were used for flux calibration.

3. Results

The results of photometry in the first night are shown in Figure 2 as lightcurves with respect to time and phase angle. The data points and error bars represent the averaged magnitude over every minute and its standard deviation, respectively. The mean uncertainty is 0.04 mag. The magnitude was adjusted for the heliocentric and geocentric distances to those at the closest approach to the Earth. The brightness reached a peak at the minimal phase

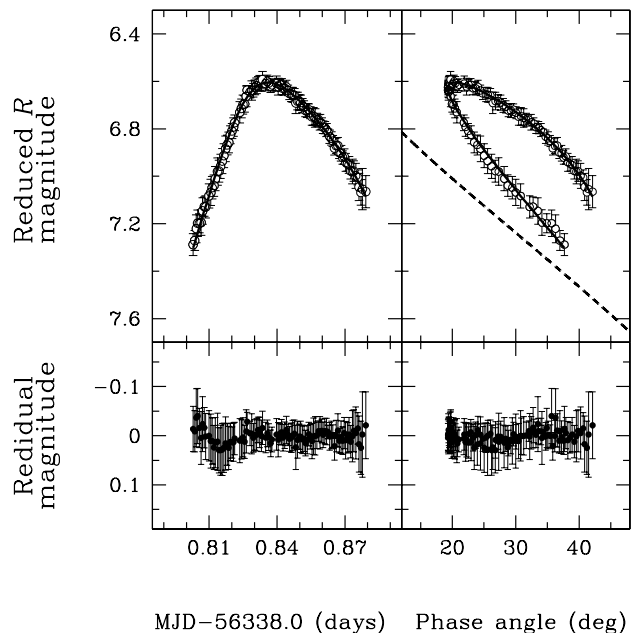


Fig. 2. The brightness variations of 2012 DA₁₄ around the closest approach at 19:33 UT on February 15, 2013 (MJD 56338.8146). The upper left and upper right panels show the lightcurve with time and solar phase angle, respectively. The open circles and solid line represent the photometric data and the best-fit model generated by a combination of the H-G phase function. The dashed line in the upper right panel represents the model phase function with $G = 0.44$, which was derived from our best-fit model. The lower left and lower right panels show the residual to the best-fit model of the lightcurves with time and solar phase angle, respectively. In the all panels, the error bars indicate the 1σ photometric uncertainties.

angle, indicating that the lightcurve was dominated by the phase effect. However, there is a discrepancy between the phase curves before and after the peak. This is likely to be due to the rotational variation in brightness, as discussed in Section 4.

Figure 3 shows the lightcurve from the second night data. The data points and error bars represent the averaged magnitude over every 3 min and its standard deviation, respectively. The mean uncertainty is 0.05 mag. The magnitude was adjusted for the heliocentric and geocentric distances to those at the beginning of the observation. Because the variation in phase angle is negligible over the observation time of the second night (82.2° – 82.6°), the lightcurve shows the brightness change caused by the asteroid’s rotation. We have analysed the lightcurve using the Lomb-Scargle periodogram technique (Lomb 1976; Scargle 1982). Figure 4 shows the resulting periodogram that indicates the plausible apparent period of around 5 hr. The synthetic curve was determined by fitting the forth-order Fourier series formulation. The best-fit model gives an apparent period of $5.5^{+0.9}_{-0.3}$ hr with a peak-to-peak amplitude of 1.59 ± 0.02 mag, where the uncertainties correspond to 1σ . Assuming a double-peaked lightcurve, we obtained the rotational period of $11.0^{+1.8}_{-0.6}$ hr. The best-fit model and its residual are shown in Figure 3.

De León et al. (2013) presented the rotational lightcurve of 2012 DA₁₄ covering from 56338.85 to 56339.20 in modified Julian date (MJD), which has some discontinuities and sharp turns. They obtained a rotational period of 8.95 ± 0.08 hr. The shape of our lightcurves and around the second maximum at MJD 56339.12 in de León et al. (2013) match each other. How-

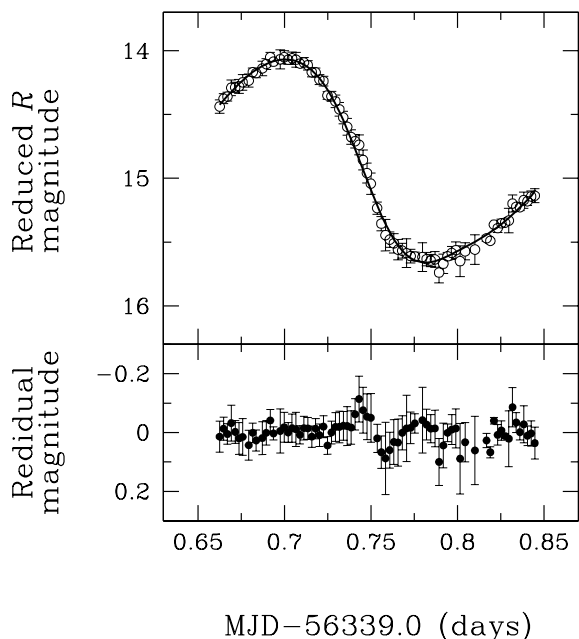


Fig. 3. The obtained lightcurve of 2012 DA₁₄ on February 16, 2013 UT. The upper panel shows the photometric data (open circles) and the best-fit model with a Fourier series curve (solid line). The lower panel shows the residual of the best-fit model. In the both panels, the error bars indicate the 1σ photometric uncertainties.

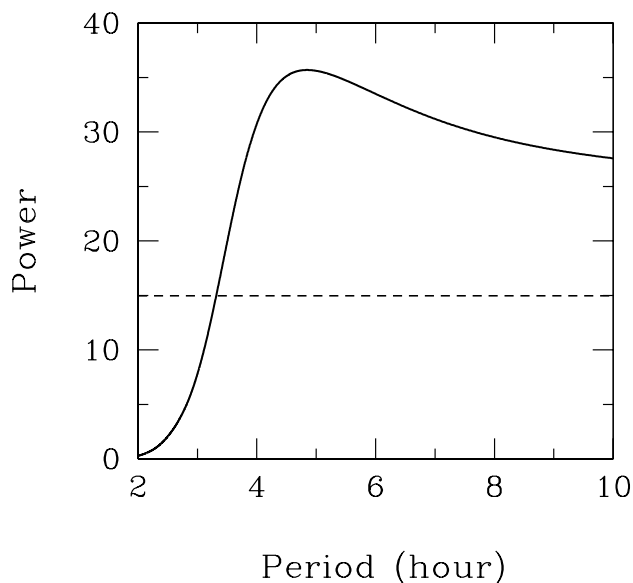


Fig. 4. Periodogram of the photometric data for 2012 DA₁₄ obtained at February 16, 2013 UT. The dashed line shows the 99.99% confidence level.

ever, we could not find the rotation period of 8.95 hr in the combined lightcurve that was derived from our observations and those of de León et al.. We note that our lightcurve was acquired when the asteroid was moving slowly and the solar phase angle was almost constant, or in good condition for precise measurement of the rotational brightness variation without

Table 1. Parameters of the best-fit model for the lightcurve of 2012 DA₁₄ around its closest approach.

Phase function	Slope parameter	H_R^a (mag)	Amplitude ^b (mag)	χ^2
Linear	$b=0.022_{-0.001}^{+0.002}$	$25.02_{-0.08}^{+0.07c}$	1.00 ± 0.04	12.6
H, G	$G=0.44_{-0.08}^{+0.06}$	$24.78_{-0.09}^{+0.11}$	1.02 ± 0.02	12.2
H, G ₁₂	$G_{12}=0.05_{-0.02}^{+0.02}$	$24.64_{-0.08}^{+0.08}$	0.90 ± 0.05	18.3

Notes. ^(a) Absolute magnitude in the R -band. ^(b) Peak-to-peak amplitude of the rotational lightcurve. ^(c) This value has been overestimated because the non-linear brightness increase at small phase angles was ignored.

the phase effect. During de León et al.'s observation on February 15, however, 2012 DA₁₄ still had a rapid sky motion ($1\text{--}20$ arcmin min^{-1}) and a significant change in the phase angle ($50^\circ\text{--}75^\circ$). These observational difficulties might have caused the inconsistent lightcurve with our result. Another possibility is that the asteroid might have experienced a significant spin down in the time during the close encounter with Earth. We adopted $11.0_{-0.6}^{+1.8}$ hr as the most probable rotational period of 2012 DA₁₄, although shorter periods cannot be ruled out.

4. Discussion

4.1. Model fitting

To understand the brightness variation of 2012 DA₁₄ around its closest approach, as seen in Figure 2, we use synthetic models generated from a combination of a given phase function and a rotational lightcurve. The latter was based on the measurements from the data of the second night assuming no variation of the rotational period from the time around the closest approach to the second night. We note that the interval between the centered times of observations at the first and second nights are about 22 hr in length corresponding to almost exactly two rotations; that is, the surface on the similar side was observed on the both nights. The rotational period and lightcurve pattern were determined from the second night data, but the peak-to-peak amplitude was parameterized. This is because the difference in inclination of the spin axis to the line of sight between the two nights is unknown, and the brightness amplitude of an ellipsoidal body depends on the phase angle (Helfenstein & Veverka 1989).

Model fitting was performed with the following three types of empirical phase functions using chi-square minimization: (i) a linearly decreasing function expressed as $b\alpha$ where b is the linear coefficient in mag deg^{-1} and α is the solar phase angle (Shevchenko et al. 1996; Kaasalainen et al. 2003), (ii) the so-called H, G phase function with the slope parameter G (Bowell et al. 1989), and (iii) the H, G₁₂ function developed by Muinonen et al. (2010). In the first function, the non-linear (exponential) brightness increase at small phase angles ($\alpha < 10^\circ$), known as the opposition effect, was ignored because of a lack of data. The slope parameter (b , G , or G_{12}), absolute magnitude, amplitude of the rotational variation, and χ^2 value of the best-fit model with each of the phase functions are listed in Table 1. We obtained nearly identical phase curves with those three functions though the H, G phase function matched with the observation most closely. The best-fit model is shown in Figure 2. The obtained slope parameter is $G = 0.44_{-0.08}^{+0.06}$.

It is widely known that asteroid phase curves are tied to surface properties and differ for different taxonomic classes (Muinonen et al. 2002). Specifically, the slope of the phase curve in the linear part ($10^\circ \lesssim \alpha \lesssim 50^\circ$) is inversely correlated with the geometric albedo (Shevchenko et al. 1996; Belskaya & Shevchenko 2000). The asteroid 2012 DA₁₄ has been classified as an L-type asteroid (de León et al. 2013; Urakawa et al. 2013). The mean value of the geometric albedo (p_V) for L-type asteroids is $p_V = 0.14 \pm 0.04$ by AKARI (Usui et al. 2013) or 0.18 ± 0.08 by WISE (Mainzer et al. 2011), which is lower than that of S-type asteroids ($p_V = 0.23 \pm 0.07$). This indicates that L-type asteroids have steeper phase curve slopes (i.e. lower G value) than S-type asteroids regardless of the surface composition. The mean G value of S-type asteroids is 0.23 ± 0.02 (Lagerkvist & Magnusson 1990). Actually, the L-type asteroids (236) Honoria ($p_V = 0.11 \pm 0.02$), (387) Aquitania (p_V is unknown), and (980) Anacostia ($p_V = 0.14 \pm 0.03$) show the G values of -0.020 ± 0.014 , 0.02 ± 0.02 , and 0.060 ± 0.003 , respectively (Pravec et al. 2012). The typical phase curve of L-type asteroids is still unclear but is expected to have a steeper slope than that of S-type asteroids. However, the phase curve of 2012 DA₁₄ that is obtained from the best-fit model is much shallower than those of the known L-type asteroids and even S-type asteroids. This fact implies that 2012 DA₁₄ could have peculiar surface properties compared to other L-type asteroids.

4.2. Interpretation

We suggest two potential mechanisms causing the shallow phase curve of 2012 DA₁₄. One is that the surface of 2012 DA₁₄ could be coated with coarse regolith. These small asteroids have a weak gravitational field and have difficulty in retaining fine particles produced by meteorite impacts. At relatively high phase angles ($\alpha \gg 1^\circ$), asteroid phase curves are dominated by the shadow-hiding effect rather than the coherent backscattering (Belskaya & Shevchenko 2000; French et al. 2007). Given a power-law size distribution of the regolith particles, an increase in the smallest particle size widens an angular width parameter of the phase curve with the shadow-hiding effect (Hapke 1993). A lack of fine particulate regolith provides a reasonable explanation for the shallower phase curve compared to larger asteroids.

Another reason is that 2012 DA₁₄ could have a high albedo surface. As mentioned in the previous section, the slope of the asteroid phase curve in the intermediate range of the solar phase angle is known to have a close correlation with geometric albedo (Shevchenko et al. 1996; Belskaya & Shevchenko 2000). E-type asteroids with a mean albedo of 0.41 (Usui et al. 2013) have a mean b value of 0.020 ± 0.002 mag deg⁻¹ (Belskaya & Shevchenko 2000) and a mean G value of 0.45 ± 0.03 (Lagerkvist & Magnusson 1990). The best-fit b and G values are consistent with those values, indicating that the albedo of 2012 DA₁₄ is as high as E-type asteroids. Using the empirical correlation between the b value and visible geometric albedo, as given by Belskaya & Shevchenko (2000), the albedo of 2012 DA₁₄ is expected to be $p_V = 0.42 \pm 0.03$. De León et al. (2013) also presented a similar albedo of 2012 DA₁₄ with a value of $p_V = 0.44 \pm 0.20$ though the uncertainty is large. These high albedo values of 2012 DA₁₄ disagree with the fact that it is a member of L-type asteroids with a typical albedo less than 0.20.

Generally, small asteroids seem to be covered by a young surface. These S-type asteroids have a surface with less reddening/darkening effects due to space weathering processes. Considering that the collisional lifetime for main-belt asteroids smaller

than 50 m in diameter is less than 10 Myr (O’Brien & Greenberg 2005), the migration from the main-belt resonances to Earth-crossing orbits is 0.1–1 Myr, and the typical dynamical lifetime of Earth-crossing NEOs is ~ 1 Myr (Gladman et al. 1997), the age of 2012 DA₁₄ is likely to be several Myr. In S-type asteroids, the timescale of the surface maturation is suggested to be 10^5 – 10^6 yr (Vernazza et al. 2009; Shestopalov et al. 2013). However, it is unclear how the reddening/darkening effects proceed on the surface of L-type asteroids. We cannot assess the relation between the albedo and surface age for 2012 DA₁₄. One possible cause we can point out is the resurfacing effect, which occurs when planetary encounters freshen asteroid surfaces by tidal stress (Binzel et al. 2010). The asteroid 2012 DA₁₄ has frequent close approaches to the Earth (Włodarczyk 2012). If this mechanism effectively acts on 2012 DA₁₄, its surface could keep high albedo.

In summary, we found that 2012 DA₁₄ rotates with at least an 11-hr period since the last Earth flyby. The asteroid shows a significantly shallow phase curve which is inconsistent with known L-type asteroids. Such an unusual phase curve indicates that 2012 DA₁₄ is covered with a coarse and/or bright surface. This result provides useful clues for understanding the origins and evolutions of asteroid surface properties and developing Spaceguard strategies.

Acknowledgements. This study is based on data collected at Saitama University observatory. We thank Yusuke Takahara, Daichi Takai, Aiko Enomoto, and Kaori Nakazato for their help during our observations. This work was supported by JSPS Grants-in-Aid for Scientific Research 25870124 from MEXT.

References

- Belskaya, I. N., & Shevchenko, V. G. 2000, *Icarus*, 147, 94
 Binzel, R. P., Morbidelli, A., Merouane, S., et al. 2010, *Nature*, 463, 331
 Bowell, E., Hapke, B., Domingue, D., et al. 1989, in *Asteroids II*, ed. R. P. Binzel et al. (University of Arizona Press, Tucson), 524
 Delbó, M., Harris, A. W., Binzel, R. P., Pravec, P., & Davies, J. K. 2003, *Icarus*, 166, 116
 de León, J., Ortiz, J. L., Pinilla-Alonso, N., et al. 2013, *A&A*, 555, L2
 French, R. G., Verbitser, A., Salo, H., McGhee, C., & Dones, L. 2007, *PASP*, 119, 623
 Gladman, B. J., Migliorini, F., Morbidelli, A., et al. 1997, *Science*, 277, 197
 Hapke, B. 1993, in *Theory of Reflectance and Emittance Spectroscopy* (Cambridge University Press, New York)
 Helfenstein, P., & Veverka, J. 1989, in *Asteroids II*, ed. R. P. Binzel et al. (University of Arizona Press, Tucson), 557
 Kaasalainen, S., Piironen, J., Kaasalainen, M., et al. 2003, *Icarus*, 161, 34
 Lagerkvist, C.-I., & Magnusson, P. 1990, *A&AS*, 86, 119
 Lomb, N. R. 1976, *Ap&SS*, 39, 447
 Mainzer, A., Grav, T., Masiero, J., et al. 2011, *ApJ*, 741, 90
 Monet, D. G., Levine, S. E., Canzian, B., et al. 2003, *AJ*, 125, 984
 Morrison, D., Harris, A. W., Sommer, G., Chapman, C. R., & Carusi, A. 2002, *Asteroids III*, ed. W. F. Bottke Jr. et al. (University of Arizona Press, Tucson), 739
 Muinonen, K., Piironen, J., Shkuratov, Y. G., Ovcharenko, A., & Clark, B. E. 2002, in *Asteroids III*, ed. W. F. Bottke Jr. et al. (University of Arizona Press, Tucson), 123
 Muinonen, K., Belskaya, I. N., Cellino, A., et al. 2010, *Icarus*, 209, 542
 O’Brien, D. P., & Greenberg, R. 2005, *Icarus*, 178, 179
 Pravec, P., Harris, A. W., Kušnirák, P., Galád, A., & Hornoch, K. 2012, *Icarus*, 221, 365
 Scargle, J. D. 1982, *ApJ*, 263, 835
 Shestopalov, D. I., Golubeva, L. F., & Cloutis, E. A. 2013, *Icarus*, 225, 781
 Shevchenko, V. G., Chiorny, V. G., Kalashnikov, A. V., et al. 1996, *A&AS*, 115, 475
 Urakawa, S., Fujii, M., Hanayama, H., et al. 2013, arXiv:1306.2111
 Usui, F., Kasuga, T., Hasegawa, S., et al. 2013, *ApJ*, 762, 56
 Vernazza, P., Binzel, R. P., Rossi, A., Fulchignoni, M., & Birlan, M. 2009, *Nature*, 458, 993
 Włodarczyk, I. 2012, *MNRAS*, 427, 1175